Inorganic Chemistry

pubs.acs.org/IC

Article

Methane Generation and Reductive Debromination of Benzylic Position by Reconstituted Myoglobin Containing Nickel Tetradehydrocorrin as a Model of Methyl-coenzyme M Reductase

Yuta Miyazaki, Koji Oohora,* and Takashi Hayashi*

Cite This: https://dx.doi.org/10.1021/acs.inorgchem.0c00901

Read Online

ACCESS | Metrics & More | Article Recommendations | Supporting Information

ABSTRACT: Methyl-coenzyme M reductase (MCR), which contains the nickel hydrocorphinoid cofactor F430, is responsible for biological methane generation under anaerobic conditions via a reaction mechanism which has not been completely elucidated. In this work, myoglobin reconstituted with an artificial cofactor, nickel(I) tetradehydrocorrin (Ni^{I}(TDHC)), is used as a protein-based functional model for MCR. The reconstituted protein, rMb(Ni^{I}(TDHC)), is found to react with methyl donors such as methyl *p*-toluenesulfonate and trimethylsulfonium iodide with methane evolution observed in aqueous media containing dithionite. Moreover, rMb(Ni^{I}(TDHC)) is found to convert benzyl bromide derivatives to reductively debrominated products without homocoupling products. The reactivity increases in the order of primary > secondary > tertiary benzylic carbons, indicating steric effects on the reaction of the nickel center with the benzylic carbon in the initial step. In addition, Hammett plots using a series of *para*-substituted benzyl bromides exhibit enhancement of the reactivity with introduction of electron-withdrawing substituents, as shown by the positive slope against polar substituent constants. These results suggest a nucleophilic S_N2-type reaction of the Ni(I) species with the benzylic carbon to provide an organonickel species as an intermediate. The reaction in D_2O buffer at pD 7.0 causes a complete isotope shift of the product by +1 mass unit, supporting our proposal that protonation of the organonickel intermediate occurs during product formation. Although the turnover numbers are limited due to inactivation of the cofactor by side reactions, the present findings will contribute to elucidating the reaction mechanism of MCR-catalyzed methane generation from activated methyl sources and dehalogenation.

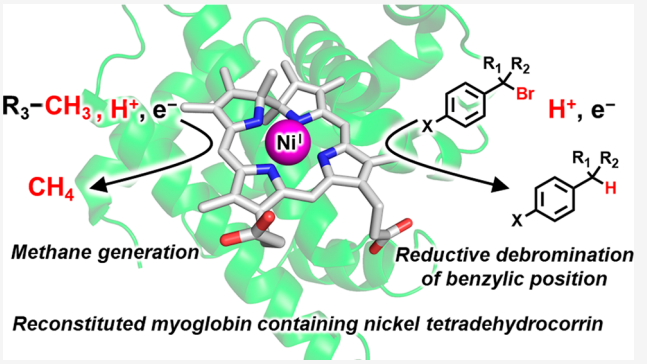

INTRODUCTION

Methyl-coenzyme M reductase (MCR), which has three different subunits forming a heterohexameric structure $(\alpha\beta\gamma)_2$, is known to contribute to the rate-determining and final step for methane formation in methanogenic archea.[1−4] Furthermore, the similar types of proteins with MCR are reported to catalyze the reverse reaction of the last step of methanogenesis, which is proposed as a first step of anaerobic oxidation of methane in a consortium that includes archaea to promote methane oxidation and microbes to couple the methane-derived electrons with reduction of an electron acceptor such as sulfate.[1−4] The active site of MCR has an F430 cofactor, a natural nickel porphyrinoid consisting of the most saturated type of monoanionic tetrapyrrole framework which is known as hydrocorphine (Figure 1a). Previous studies have demonstrated that the redox active behavior of F430 involves the Ni(I), Ni(II), and Ni(III) oxidation states.[5] In methane generation, MCR catalyzes the conversion of methyl-coenzyme M (CH_3S−CoM) and coenzyme B (HS−CoB) to methane and a heterodisulfide (CoM−S−S−CoB) using the active Ni(I) species of F430 (Figure 1b). MCR and F430 itself also promote dechlorination of alkyl chlorides as well as reductive dehalogenation of alkyl iodide, brominated acids, and bromoalkanesulfonates to produce alkanes, alkanoic acids and alkanesulfonates, respectively.[6,7] The results of extensive theoretical and experimental studies have led to proposals of two plausible reaction mechanisms in the methane generation reaction including either a CH_3−Ni(III) intermediate or a transient methyl radical species.[1−3] The former intermediate is estimated to be generated by a nucleophilic attack of the Ni(I) species on the methyl group of the thioether moiety of methyl-coenzyme M, followed by further electron transfer and proton transfer from coenzyme M to achieve methane generation. This reaction mechanism is supported by the results of crystallographic and mechanistic investigations based on

Received: March 26, 2020

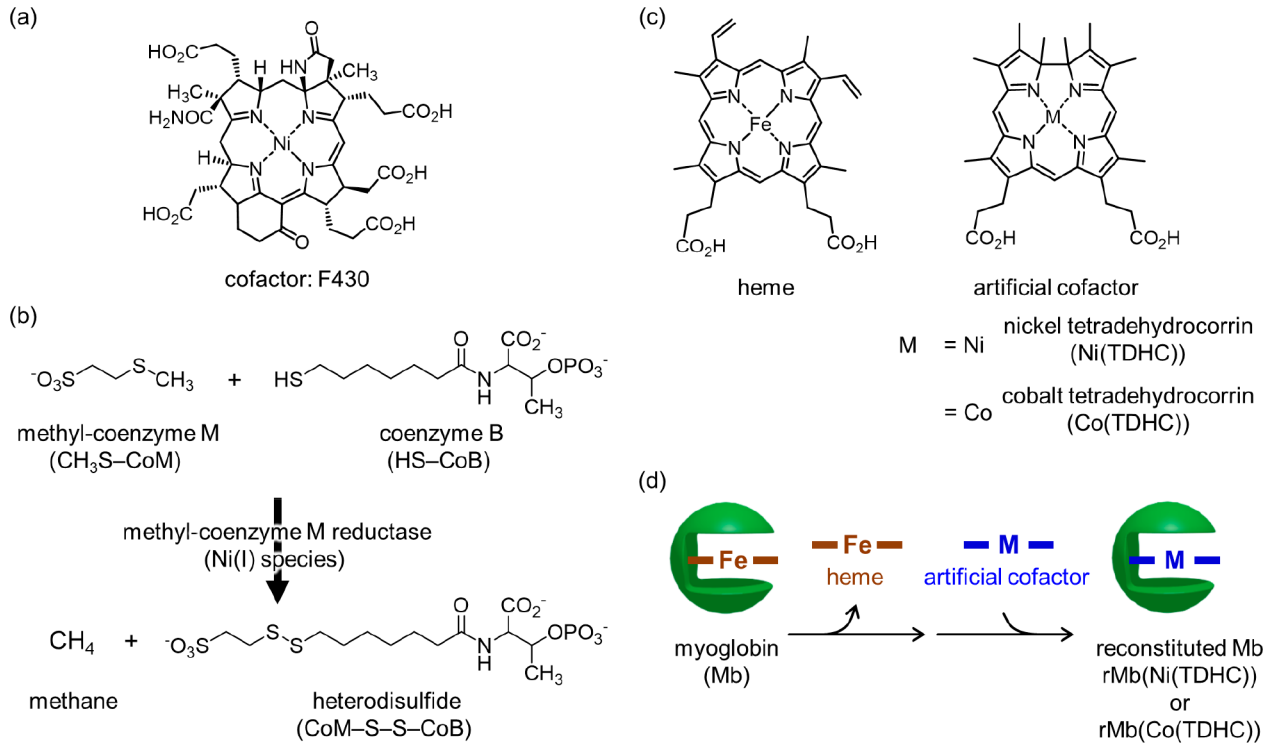

Figure 1. (a) Chemical structure of F430. (b) Methyl-coenzyme M reductase catalyzing methane formation reaction in methanogenic archaea. (c) Chemical structures of heme and artificial cofactors. (d) Schematic representation of the reconstitution of myoglobin with artificial cofactors.

reactions of the Ni(I) species in MCR[7−9] or F430 model complexes[10−12] with activated alkyl reagents, especially alkyl bromides and iodides via formation of (alkyl)C−Ni(III) species.[7] In the latter case, the transitional methyl radial species is believed to be generated by homolytic cleavage of the C−S bond of methyl-coenzyme M promoted by the Ni(I) species, and then a hydrogen atom of coenzyme B is abstracted to generate methane gas. This mechanism is supported by theoretical investigations[13] and, more recently, a single turnover reaction using the active Ni(I) species in MCR with less reactive coenzyme analogues.[14]

Model complexes of F430 which have been investigated include nickel porphyrinoids,[10,11,15] nickel azacyclam complexes,[12,16,17] and a cobalamin-based nickel complex.[18] Nickel(II) octaethylisobacteriochlorin (Ni(OEiBC)), which has more saturated tetrapyrrole framework compared with porphyrin, is a suitable model because Ni(OEiBC) can be quantitatively reduced to a Ni(I) species in organic solvents (Figure S1).[10,11] The electrochemically and chemically prepared Ni(I) species (Ni^{I}(OEiBC)$^{-}$) demonstrates reactivity similar to that of pentamethyl ester of F430 (F430M) and promotes reactions with alkyl halides such as methyl halides and benzyl halide derivatives to produce reductively dehalogenated and homocoupling compounds. Mechanistic studies based on spectroscopic and electrochemical kinetic studies and product analyses indicate that the initial step occurs in a nucleophilic S_N2-type mechanism to form an organometallic (alkyl)C−Ni(III) intermediate and the second step, the product formation step, follows the protonation in an ionic mechanism or hydrogen abstraction in a radical-based mechanism depending on the polarity of organic solvents.[10,11] However, the reactive (alkyl)C−Ni(III) intermediate could not be isolated and identified and the Ni(I) species is unstable in aqueous media. In contrast, the protein matrix of MCR plays an important role in promoting and regulating the enzymatic reaction, although essentially all of the model complexes have not been considered in terms of mimicking the effect of the protein matrix. Our group has recently developed protein-based functional models of heme, cobalamin, and F430-depedent enzymes by conjugation of appropriate model complexes with apo-forms of simple and robust hemoproteins such as myoglobin and cytochrome b_{562} which have hydrophobic cavities for cofactor binding. These hemoprotein-based models replicate the physicochemical properties and reactivities of the enzymes under physiological conditions and are used to evaluate the effects of the protein matrix in the enzymatic reactions.[19,20] Recently, nickel(II) tetradehydrocorrin (Ni^{II}(TDHC)) (Figure 1c) was synthesized as a model of F430 and found to have a positively shifted redox potential for the Ni^{II}/Ni^{I} redox process. The finding that this model is reducible with a mild reductant such as dithionite is advantageous because native F430 and other model systems require strong reductants such as Na/Hg and Ti(III) citrate.[20a] Ni(OEiBC), an aforementioned useful model of F430, has redox potential that is 940 mV more negative for the Ni^{II}/Ni^{I} couple than that for the corresponding redox potential of Ni(TDHC) because of the dianionic feature of the OEiBC ligand in contrast to monoanionic hydrocorphine and TDHC ligands.[10a,20a] Furthermore, insertion of Ni^{I}(TDHC) into the apo-form of myoglobin (Mb) provides reconstituted Mb (rMb(Ni^{I}(TDHC))) as a protein-based functional model of MCR (Figure 1d). The functional model demonstrates sufficient reactivity for conversion of methyl iodide to methane gas, whereas Ni^{I}(TDHC) without the protein matrix generates a negligible amount of methane gas.[20a] This finding indicates the importance of the protein matrix in the reaction. Spectroelectrochemical measurements suggest that the protein matrix may increase the reactivity of the Ni(I) species as a

https://dx.doi.org/10.1021/acs.inorgchem.0c00901
Inorg. Chem. XXXX, XXX, XXX−XXX

result of axial coordination of the proximal histidine residue, His93, to the nickel center.[20a] Given the fact that rMb-(Ni^{I}(TDHC)) reacts with methyl iodide to produce methane gas as seen in MCR, further investigation of rMb-(Ni^{I}(TDHC)) using other model substrates is expected to be a useful strategy for elucidating the reaction mechanism of MCR. In the present study, we report the reactivity of rMb(Ni^{I}(TDHC)) in aqueous solution with respect to various methyl donors in the methane generation reaction and with respect to benzyl bromide derivatives in the reductive debromination reaction. Product distribution analysis and evaluation of the substituent effect of benzyl bromide derivatives provide essential understanding to realize the nucleophilicity of the Ni(I) species and the S_N2-type reaction mechanism for reactive alkyl halides.

RESULTS AND DISCUSSION

Methane Gas Generation from Methyl Donors. Reactions of methyl donors with rMb(Ni^{I}(TDHC)) to generate methane were carried out in potassium phosphate buffer at pH 7.0 and 25 °C in the presence of dithionite under an N_2 atmosphere. Dithionite was employed as a reductant in contrast to the strong reductants Na/Hg or Ti(III) citrate which were used in investigations of previous model complexes.[10,11,15] Generated gases were identified and quantified by GC. Table 1 summarizes the amount of methane

Table 1. Products of the Reaction of rMb(Ni^{I}(TDHC)) with Methyl Donors[a,b,c]

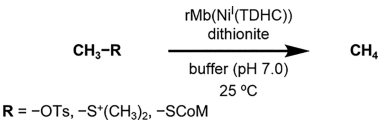

substrate	methane (nmol)	TON for methane	ethane (nmol)	TON for ethane
methyl *p*-toluenesulfonate[a]	2.2 ± 0.32	0.099 ± 0.014	n.d.	-
trimethylsulfonium iodide[a]	2.0 ± 0.36	0.087 ± 0.016	n.d.	-
methyl-coenzyme M[a]	n.d.	-	n.d.	-
methyl iodide[b]	36.2 ± 0.92	1.61 ± 0.041	n.d.	-

[a]General reaction conditions: [rMb(Ni^{I}(TDHC))] = 45 μM, [dithionite] = 1.0 mM, [methyl donors] = 5.0 mM in potassium phosphate buffer (100 mM, pH 7.0) at 25 °C for 7 h under an N_2 atmosphere. Products were identified and quantified by GC. [b]Ref 20a. Reaction conditions: [rMb(Ni^{I}(TDHC))] = 45 μM, [dithionite] = 1.0 mM, [methyl iodide] = 20 mM in potassium phosphate buffer (100 mM, pH 8.0) at 25 °C for 7 h under an N_2 atmosphere. Products were identified and quantified by GC. [c]n.d.: not detected.

gas generated from methyl donors. Methane gas generation was observed in the reaction of methyl *p*-toluenesulfonate (2.2 nmol) and trimethylsulfonium iodide (2.0 nmol) (Figure S2). In contrast, control experiments using the nickel complex itself without the protein matrix and using only dithionite exhibited no methane generation (Tables S1 and S2). Methyl *p*-toluenesulfonate is known to have poor reactivity in a radical-based mechanism.[10b] Trimethylsulfonium iodide is the simplest sulfonium species with an activated C–S bond.[9a,10b,21] In both reactions, no other gases such as ethane were observed. In contrast, methyl-coenzyme M does not promote a methane generation reaction. The amounts of methane generated from methyl *p*-toluenesulfonate and trimethylsulfonium iodide with rMb(Ni^{I}(TDHC)) were less than the amounts generated by previously reported model complexes.[9a,10b,21] This could be due to steric hindrance. However, both the methane gas generation from methyl *p*-toluenesulfonate and absence of ethane gas from each substrate provide evidence that the reaction proceeds via an ionic mechanism in the present system, so a radical-based mechanism is ruled out. In the case of methyl-coenzyme M, it appears difficult for the Ni(I) species to activate the C–S bond of the thioether moiety without an appropriate reaction scaffold because F430M without the protein matrix and previous model complexes fail to generate methane from methyl-coenzyme M in spite of negative redox potentials of the Ni^{II}/Ni^{I} processes and high reactivities.[9a,10b] In native MCR, substrates and cofactor are precisely positioned in the reaction site which is located at the end of a funnel-shaped substrate channel with a length of 30 Å.[8] Crystal structure analyses have revealed that methyl-coenzyme M predominantly binds to the reaction site via a salt bridge and hydrogen bonding interactions of its sulfonate moiety with amino acid residues to direct its thioether moiety toward the front of F430. Coenzyme B also fits within the substrate channel with salt bridges formed between its threoninephosphate moiety and residues near the surface of the protein matrix, resulting in its thioheptanoyl moiety being directed toward the thioether moiety of methyl-coenzyme M and preservation of a hydrophobic environment during the enzymatic reaction to protect the highly reactive Ni(I) species from bulk solvent. Furthermore, it has been proposed that binding of substrates to appropriate positions induces a conformational change in MCR to move the methyl-coenzyme M cofactor closer to the nickel center of F430.[8b,22] Thus, the active site of MCR is highly optimized to promote the C–S bond cleavage. Although rMb(Ni^{I}(TDHC)) contains a Ni(I) species in a hydrophobic reaction site within the Mb matrix, it does not provide a completely optimized configuration to precisely arrange the substrate and induce the proximity effect observed in native MCR, causing rMb(Ni^{I}(TDHC)) to be relatively inert with respect to C–S bond cleavage. The amount of methane generated from the substrates in this study is lower than that from the previously used methyl donor, methyl iodide. This is due to the intrinsically higher reactivity of methyl iodide relative to those of methyl *p*-toluenesulfonate and trimethylsulfonium iodide. The low TON values are possibly derived from the unfavorable deactivation/decomposition of Ni-(TDHC).[20]

Reductive Debromination Reaction of Benzylic Position with Benzyl Bromide Derivatives. The results of the methane generation reaction led to the expectation that rMb(Ni^{I}(TDHC)) would be reactive toward alkyl halides and yield reductively dehalogenated compounds. Table 2 shows the results of the reaction of excess benzyl bromide and its derivatives in potassium phosphate buffer at pH 7.0 and 4 °C under an N_2 atmosphere in the presence of dithionite, followed by extraction of nonvolatile compounds with an organic solvent. The extracted compounds were analyzed by GC/MS. It was found that benzyl bromide is converted to toluene (9.8 μM) as a reductively debrominated product under conventional conditions (Tables 2 and S3). Dibenzyl, a homocoupling product generated via a radical-based mechanism, was not detected. The time-course plots of generated amounts of toluene are shown in Figure 2. The initial reaction rate

https://dx.doi.org/10.1021/acs.inorgchem.0c00901
Inorg. Chem. XXXX, XXX, XXX–XXX

Table 2. Products of the Reaction of rMb(Ni^{I}(TDHC)) with Benzyl Bromide Derivatives[a,b]

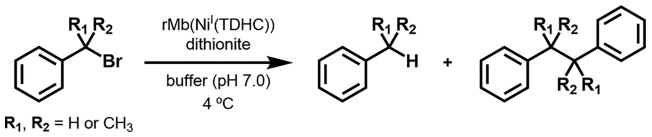

protein	substrate	reductively debrominated product (μM)[c]	TON for reductively debrominated product	homocoupling product (μM)[d]	TON for homocoupling product	k_{obs} (μM·min^{-1})[e]
rMb(Ni^{I}(TDHC))	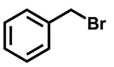 benzyl bromide	9.8 ± 0.31	0.22 ± 0.007	n.d.	-	0.39 ± 0.05
	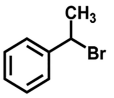 1-phenylethyl bromide	1.0 ± 0.05	0.02 ± 0.001	n.d.	-	0.057 ± 0.005
	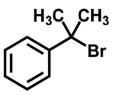 cumyl bromide	n.d.	-	n.d.	-	-
rMb(Co^{I}(TDHC))	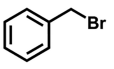 benzyl bromide	11.1 ± 0.11	0.25 ± 0.002	0.5 ± 0.15	0.01 ± 0.002	-

[a]General reaction conditions: [rMb(Ni^{I}(TDHC))] or [rMb(Co^{I}(TDHC))] = 45 μM, [dithionite] = 1.0 mM, [benzyl bromide derivative] = 1.0 mM in potassium phosphate buffer (100 mM, pH 7.0) containing 1% (v/v) acetonitrile at 4 °C for 2 h under an N_2 atmosphere. Products were identified and quantified by GC/MS. Acetonitrile was used as a cosolvent to dissolve the hydrophobic substrates in the water media. [b]n.d.: not detected. [c]Toluene from benzyl bromide, ethylbenzene from 1-phenylethyl bromide, and cumene from cumyl bromide. [d]Dibenzyl from benzyl bromide, 2,3-diphenylbutane from 1-phenylethyl bromide, and dicumene from cumyl bromide. [e]The values for k_{obs} were obtained as rate constant averaged in the reaction at 5 and 10 min. The constants were verified with triple independent experiments.

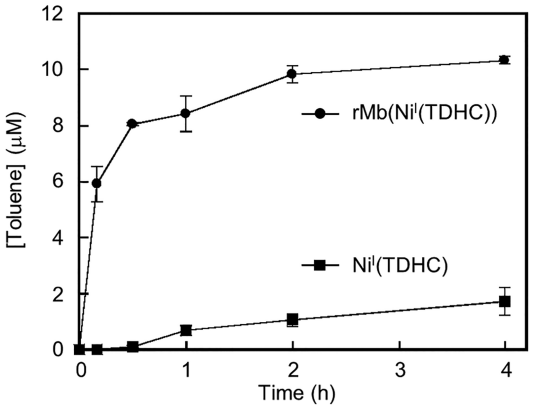

Figure 2. Time-course plots of toluene generation using rMb(Ni^{I}(TDHC)) (solid circles) or Ni^{I}(TDHC) (solid square). Conditions: [rMb(Ni^{I}(TDHC))] or [Ni^{I}(TDHC)] = 45 μM, [dithionite] = 1.0 mM, [benzyl bromide] = 1.0 mM in potassium phosphate buffer (100 mM, pH 7.0) containing 1% (v/v) acetonitrile at 4 °C under an N_2 atmosphere.

constant, k_{obs}, for the production of toluene was determined in the reaction within 10 min (Figure S3). rMb(Ni^{I}(TDHC)) provides 9.8 μM toluene with k_{obs} of 0.39 μM·min^{-1}, whereas bare Ni^{I}(TDHC) generates significantly less toluene. This indicates the importance of the protein matrix in the reaction. The protein matrix appears to cause a redox shift in the Ni^{II}/Ni^{I} process as a result of the axial histidine coordination to the nickel center as suggested in our previous report.[20a] Toluene generation was found to be essentially saturated within 2 h possibly due to a side reaction causing deactivation and/or decomposition of rMb(Ni^{I}(TDHC)). ESI-TOF mass spectral analysis of rMb(Ni^{I}(TDHC)) after the reaction reveals that the protein matrix and Ni(TDHC) are modified with several benzyl groups (Figure S4).[23,24] The addition of benzyl bromide to rMb(Ni^{I}(TDHC)) aqueous solution initiates rapid UV−vis spectral changes with the disappearance of peaks at 501 and 598 nm and the appearance of a new peak at 557 nm (Figure 3a). The transiently formed reaction intermediate appears to be a (benzyl)C−Ni(III) species which is immediately transformed to the inactivated benzyl group adduct. The existence of a similar intermediate species

https://dx.doi.org/10.1021/acs.inorgchem.0c00901
Inorg. Chem. XXXX, XXX, XXX−XXX

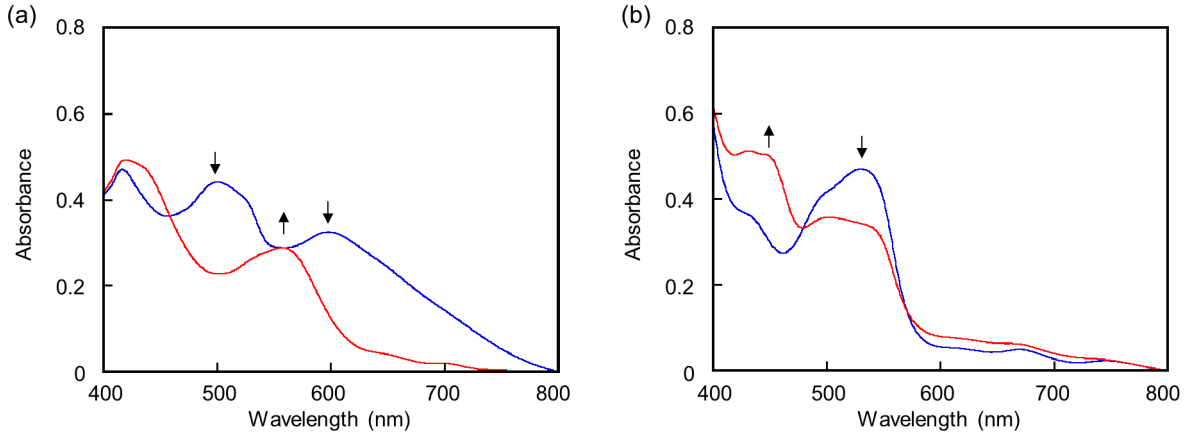

Figure 3. UV−vis spectral changes of (a) rMb(Ni^{I}(TDHC)) and (b) rMb(Co^{I}(TDHC)) before (blue line) and after (red line) addition of benzyl bromide in potassium phosphate buffer (100 mM, pH 7.0) containing 1% (v/v) acetonitrile and 1.0 mM dithionite at 4 °C under an N_2 atmosphere.

has been suggested to be included in the reaction of Ni^{I}(OEiBC)$^{-}$ with alkyl halides.[10,11] The red profile monitored by UV−vis spectroscopy is possibly assigned as a cofactor-benzyl adduct linked at the meso position. The modified cofactor by the benzyl group is expected to be irreducible with dithionite because of the undesired redox potential shift.[23] Furthermore, the modified cofactor may no longer be present in the protein matrix due to the steric hindrance, although there is no experimental information.

Other benzyl bromide derivatives, 1-phenylethyl bromide and cumyl bromide, were also investigated as substrates for debromination with rMb(Ni^{I}(TDHC)) (Table 2). The reaction of 1-phenylethyl bromide afforded only ethylbenzene (1.0 μM) as a product. The reaction rate constant for ethylbenzene generation was determined to be 0.057 μM·min^{-1}. This rate constant is about 7-fold less than the rate constant determined for the reaction with benzyl bromide. Moreover, cumyl bromide is not converted by rMb(Ni^{I}(TDHC)), and neither cumene nor dicumene was detected at all. The reactivities of a series of benzyl bromide derivatives increase in the order of primary > secondary > tertiary benzylic carbons, indicating steric effects on the reaction with the nickel center in the initial step.[10b,11] Assuming the initial reaction follows a radical-based mechanism, the reaction rate constants should increase in the reverse order because of the stability of the alkyl radical.[16] Thus, these results indicate that the Ni(I) species attacks the benzylic position in a nucleophilic S_N2-type reaction in the initial step, which is consistent with the previously suggested mechanism for the reaction of Ni^{I}(OEiBC)$^{-}$ with activated alkyl reagents.

Debromination Reaction of Benzyl Bromide Using Cobalamin Model System. The vitamin B_{12} derivative known as cobalamin is a cobalt complex with a monoanionic corrin ligand which catalyzes dehalogenation reactions.[6,25] The dehalogenation reaction of alkyl halides proceeds via the following three steps: (1) reduction of the Co(III) species to the Co(I) species, (2) reaction of the Co(I) species with an electrophilic halide, and (3) homolytic cleavage of the C−Co bond to form an alkyl radical species, which provides a reductively dehalogenated product or dimerized compound by homocoupling.[25b] In our previous work, Mb reconstituted with cobalt tetradehydrocorrin, rMb(Co(TDHC)), was evaluated as a protein-based functional model of a cobalamin-dependent enzyme (Figures 1cd).[26] We decided that rMb(Co^{I}(TDHC)) would be a suitable catalyst to compare with rMb(Ni^{I}(TDHC)). The debromination reaction of benzyl bromide using rMb(Co^{I}(TDHC)) provides both toluene and dibenzyl in which the formation of dibenzyl indicates distinctive evidence of the radical-based mechanism in the product formation step (Table 2). The homocoupling product was obtained as a minor product possibly due to the ease of hydrogen abstraction from the protein matrix within rMb(Co^{I}(TDHC)), because the concentration of the radical in the solution will generally dominate the product distribution.[27] The addition of benzyl bromide to a solution of rMb(Co^{I}(TDHC)) in phosphate buffer (pH 7.0) leads to characteristic UV−vis spectral changes with the disappearance of a peak at 530 nm and the appearance of new peaks at 448 and 497 nm as well as shoulders at 430 and 545 nm. Indeed, the spectrum after the reaction is assumed to indicate formation of a (benzyl)C−Co(III) species in a protein matrix according to its similarity with that of the CH_3−Co(III) species in which peaks at 425 and 445 nm are formed upon addition of methyl iodide to rMb(Co^{I}(TDHC)).[26] Taken together, the reductive debromination of benzyl bromide using rMb(Co^{I}(TDHC)) appears to proceed via the radical-based mechanism which includes homolytic cleavage of the C−Co bond of the organometallic (benzyl)C−Co(III) species, resulting in the formation of the homocoupling product. This reaction is sharply different from the reaction observed for rMb(Ni^{I}(TDHC)), which does not produce dibenzyl derivatives derived from the generation of radical species.[28]

Evaluation of Substituent Effect of Benzyl Bromide Derivatives. For further evaluation of the reductive debromination reactivity of rMb(Ni^{I}(TDHC)), reactions with a series of *para*-substituted benzyl bromides with methyl-, iodo-, bromo-, chloro-, trifluoro-, cyano-, and nitro-groups were investigated.[29] The corresponding toluene derivatives produced by reductive debromination were quantified by GC/MS (Figure S5). The k_{obs} values for generation of the toluene derivatives are summarized in Table S4.

Benzyl bromide derivatives with electron-withdrawing substituents (e.g., −CN and $-NO_2$) and electron-donating substituent (e.g., $-CH_3$) were found to exhibit higher and lower reaction rate constants, respectively, compared to that of benzyl bromide. Plots of the log k_{obs} values against the values

https://dx.doi.org/10.1021/acs.inorgchem.0c00901
Inorg. Chem. XXXX, XXX, XXX−XXX

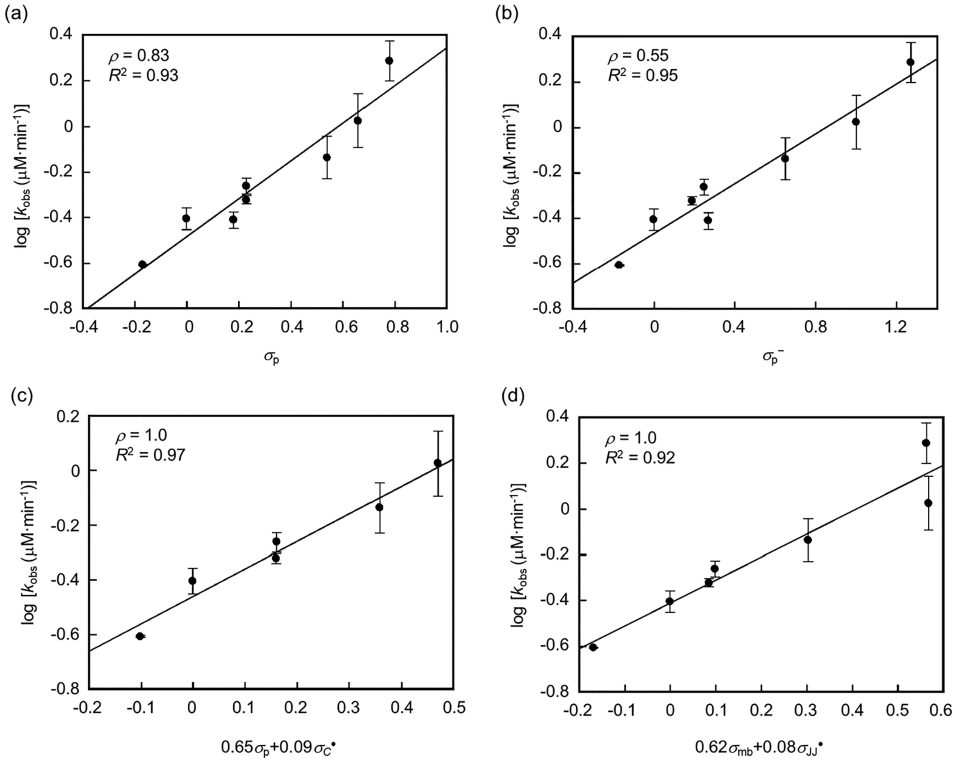

Figure 4. Plots of log k_{obs} vs σ_P (a), σ_P^- (b), $0.65\sigma_P + 0.09\sigma_C^\bullet$ (c), and $0.62\sigma_{mb} + 0.08\sigma_{JJ}^\bullet$ (d) for the reductive debromination reaction of *para*-substituted benzyl bromides ($-CH_3$, $-H$, $-I$, $-Br$, $-Cl$, $-CF_3$, $-CN$, and $-NO_2$) by rMb(Ni^I(TDHC)).

of the Hammett σ_P substituent constant[30] show a strong linear correlation with the ρ_P value of +0.83 (R^2 = 0.93) (Figure 4a). Employment of the resonance-responsive Hammett σ_P^- substituent constant[30] slightly improves the correlation among other σ polar substituent constants to yield a ρ_P^- value of 0.55 (R^2 = 0.95), whereas several σ spin-delocalization substituent constants give low linear correlations (R^2 = 0.50 for $\sigma_J^\bullet$,[31] 0.35 for $\sigma_{JJ}^\bullet$,[32] 0.46 for $\sigma_C^\bullet$,[33,34] 0.24 for $\sigma_\alpha^\bullet$,[35] and 0.71 for $\sigma_F^\bullet$[36]) (Figures 4b, S6, and S7). The positive ρ values with σ polar substituent constants (ρ_P = 0.83 and ρ_P^- = 0.55) indicate the formation of a negatively charged transition state at the rate-determining step and rule out a dominant contribution of the radical-based mechanism. To take into account both the polar effect ($\rho^X\sigma^X$) and the spin-delocalization effect ($\rho^\bullet\sigma^\bullet$) of the substituents, we employed a dual-parameter equation [log k_{obs} = $\rho^X\sigma^X$ + $\rho^\bullet\sigma^\bullet$].[37,38] Plotting the data with the Hammett σ_P substituent constant and Creary's $\sigma_C^\bullet$ spin-delocalization substituent constant in a multiple linear regression provides ρ_P and $\rho_C^\bullet$ values of +0.65 and +0.09, respectively, with the a significantly improved linear correlation (R^2 = 0.97) as well as the result using Jiang's σ_{mb} polar substituent constant[39] and $\sigma_{JJ}^\bullet$ spin-delocalization substituent constant (ρ_{mb} = +0.62, $\rho_{JJ}^\bullet$ = +0.08, R^2 = 0.92) (Figures 4cd). The large $|\rho^X/\rho^\bullet|$ ratios of 7.2 ($\rho_P/\rho_C^\bullet$) and 7.8 ($\rho_{mb}/\rho_{JJ}^\bullet$) indicate that the polar effect is dominant in the reductive debromination reaction of benzyl bromide by rMb(Ni^I(TDHC)). Furthermore, the positive ρ_P and ρ_{mb} values are similar to those obtained with the above-mentioned plots using single polar substituent constants. These results provide clear support for a mechanism which includes nucleophilic attack of the Ni(I) species on the benzylic position in the rate-determining step of the reductive debromination reaction. This is consistent with the previously reported S_N2-type mechanism in Ni^I(OEiBC)$^-$.[10,11] Although Hammett plots for S_N2-type reactions by organometallic compounds generally provide broken and curved relationships due to switching of the rate-determining step between oxidative addition and reductive elimination,[40] the continuous linear relationship obtained in the present experiments appears to exhibit an invariant rate-determining step because of the highly reactive (benzyl)C−Ni(III) intermediate.

Isotope-Labeling Experiment in the Buffer of D_2O. To obtain further insights into understanding the reaction mechanism, the reaction of rMb(Ni^I(TDHC)) with benzyl bromide was carried out in a solution of D_2O (pD 7.0 in phosphate buffer) at 4 °C for 2 h under an N_2 atmosphere. Analysis of the extracted products by GC/MS indicates that the peak obtained at the same retention time as that of authentic toluene (Figure S8a) is shifted quantitatively by +1 mass unit, indicating the formation of toluene-d_1 (Figure S8b). The deuteration of the reductively debrominated product without detection of a dimerized product indicates that the first step of activation of benzyl bromide proceeds via an S_N2-type reaction with attack of the Ni(I) species on the benzylic position to transiently form the (benzyl)C−Ni(III) species followed by the product formation step via the ionic mechanism which includes protonation.

CONCLUSIONS

In conclusion, it is found that the reaction of rMb(Ni^I(TDHC)) with methyl *p*-toluenesulfonate and trimethylsulfonium iodide in the presence of dithionite leads to methane gas generation in aqueous media, although previously reported model complexes of F430 require a strong reductant in organic solvent. In addition, rMb(Ni^I(TDHC)) converts benzyl bromide derivatives to reductively debrominated products

https://dx.doi.org/10.1021/acs.inorgchem.0c00901
Inorg. Chem. XXXX, XXX, XXX−XXX

with characteristic reactivity, which decreases with increasing the steric hindrance at the benzylic position and does not provide a homocoupling product. Furthermore, the heme pocket of myoglobin plays an important role in promoting these reactions because the products are not formed by protein-free Ni(TDHC) under the same conditions. Hammett plots for the reaction with *para*-substituted benzyl bromides provide support for the ionic reaction mechanism, which occurs via a negatively charged transition state. Evidence for this proposed mechanism is also provided by the observation that benzyl bromide is converted to toluene-d_1 in D_2O under the same conditions. These results indicate that the reaction of the Ni(I) species with benzyl bromide proceeds via a nucleophilic S_N2-type mechanism in the first step to form the transient organonickel intermediate followed by protonation (Figure S9). This is proposed for the productive mechanism, and the actual reaction with the low turnover numbers includes a significant nonproductive pathway to form an inactive cofactor-benzyl adduct linked at the meso position. Even though the reaction behavior of benzyl bromide is different from the reaction behavior observed for native methyl-coenzyme M which has a thioether moiety, the present study demonstrates a model reaction toward alkyl halide activations in an aqueous media. The future work on the detection and characterization of intermediates in the model will enhance our understanding of the enzymatic mechanism of MCR toward activated alkyl halides. Furthermore, the present finding provides important insights into understanding the reactivity of a low-valent nickel complex supported by a protein scaffold. This also contributes to the emergent topic to create artificial metalloenzymes catalyzing unique non-natural reactions such as carbene insertion because several abiological cofactors are known to show the outstanding reactivities within protein matrices optimized by mutagenesis.[41−44]

EXPERIMENTAL SECTION

Methane Generation Reaction. Methyl donors (methyl *p*-toluenesulfonate, trimethylsulfonium iodide, and methyl-coenzyme M) (final concentration: 5.0 mM) were combined with a solution of rMb(Ni^{I}(TDHC)) (final concentration: 45 μM) and dithionite (final concentration: 1.0 mM) dissolved in potassium phosphate buffer (100 mM, pH 7.0) or buffer containing 1% acetonitrile (v/v) in the case of methyl *p*-toluenesulfonate in a 2.0 mL vial capped with silicon septum rubber. After incubation of reaction solution (500 μL in total) at 25 °C for 7 h, an aliquot of the headspace gas (100 μL) was taken out using a Hamilton gas-tight syringe for GC analysis. Identification of the product was conducted by comparing its GC retention time with that of an authentic standard. A calibration curve obtained with an authentic standard was employed to determine the amount of generated methane gas. The determined amount of methane was further corrected with both of total headspace (1.5 mL) and calculated amount of methane gas dissolved in the solution. All the data were verified with triple independent experiments.

Reductive Debromination Reaction of Benzylic Position. Benzyl bromide or its derivative (1-phenylethyl bromide or cumyl bromide) (final concentration: 1.0 mM) was combined with a solution of rMb(Ni^{I}(TDHC)) or rMb(Co^{II}(TDHC)) (final concentration: 45 μM) and dithionite (final concentration: 1.0 mM) dissolved in potassium phosphate buffer (100 mM, pH 7.0) containing 1% (v/v) acetonitrile. The mixture (500 μL in total) was incubated at 4 °C for 2 h. After the reaction, 1,3,5-trimethoxybenzene (final concentration: 1.0 mM) was added as an internal standard, followed by extraction with 500 μL of diethyl ether. The organic layer was then analyzed by GC/MS. Identification of the product was conducted by comparing its retention time in the chromatogram and mass spectrum with those of authentic standards. The amount of product was determined with the calibration curve obtained using an authentic standard. The calibration curves were prepared including the process of the extraction of authentic standards in a buffer solution by diethyl ether to solve the artifact by distribution of the products in water and organic phases. For the time-course experiments, the reaction was quenched by exposure to the air, which immediately oxidized the active Ni(I) species, just before the extraction by diethyl ether.

To obtain data for the Hammett plots, the reactions were analyzed at 5 and 10 min after addition of *para*-substituted benzyl bromides. The values of log k_{obs} for the debromination of *para*-substituted benzyl bromides were plotted against the Hammett substituent constants as well as polar and spin-delocalization substituent constants for *para*-substituents. The values for k_{obs}, the initial rate constant, were obtained as averaged rate constants in the reaction at 5 and 10 min.

For isotope-labeling reactions, the reactions were carried out in potassium phosphate buffer (100 mM, pD 7.0 in D_2O) containing 1% (v/v) acetonitrile with incubation at 4 °C for 2 h. The pD value was calculated according to the previously reported formula.[45]

All the data were verified with triple independent experiments.

ASSOCIATED CONTENT

Supporting Information

The Supporting Information is available free of charge at https://pubs.acs.org/doi/10.1021/acs.inorgchem.0c00901.

Instruments; materials and methods; synthesis of sodium 2-methylthioethanesufonate (methyl-coenzyme M); synthesis of 2-bromo-2-phenylpropane (cumyl bromide); GC and GC/MS analyses for methane generation and reductive dehalogenation reaction; chemical structure of Ni(OEiBC); products of the reaction of Ni^{I}(TDHC) with methyl donors; products of the reaction of dithionite with methyl donors; GC traces of the reaction of rMb(Ni^{I}(TDHC)) with methyl *p*-toluenesulfonate or trimethylsulfonium iodide in the presence of dithionite; products of the reaction of rMb(Ni^{I}(TDHC)) with benzyl bromide under different pH values; time-course plots of toluene derivatives generation by the reductive dehalogenation of benzyl bromide and 1-phenylethyl bromide using rMb(Ni^{I}(TDHC)); ESI-TOF mass spectra for protein and Ni(TDHC) complex of rMb(Ni^{I}(TDHC)) after the dehalogenation reaction with benzyl bromide; values of log k_{obs} for reductive dehalogenation reaction of *para*-substituted benzyl bromides by rMb(Ni^{I}(TDHC)) and tabulated Hammett substituent constants for *para*-substituents; time-course plots of *para*-substituted toluene derivatives generation by the reductive dehalogenation of *para*-susbstituted benzyl bromides; plots of log k_{obs} vs σ_p^+ and σ_{mb} for the reductive dehalogenation reaction of *para*-substituted benzyl bromides by rMb(Ni^{I}(TDHC)); plots of log k_{obs} vs $\sigma_J^{\bullet}$, $\sigma_{JJ}^{\bullet}$, $\sigma_C^{\bullet}$, $\sigma_\alpha^{\bullet}$, and $\sigma_F^{\bullet}$ for the reductive dehalogenation reaction of *para*-substituted benzyl bromides by rMb(Ni^{I}(TDHC)); GC/MS traces of the reaction using benzyl bromide and mass spectra of generated toluene; and suggested reaction mechanisms (PDF)

AUTHOR INFORMATION

Corresponding Authors

Koji Oohora − *Department of Applied Chemistry, Graduate School of Engineering, Osaka University, Suita 565-0871,*

https://dx.doi.org/10.1021/acs.inorgchem.0c00901
Inorg. Chem. XXXX, XXX, XXX−XXX

Japan; orcid.org/0000-0003-1155-6824; Email: oohora@chem.eng.osaka-u.ac.jp

Takashi Hayashi − *Department of Applied Chemistry, Graduate School of Engineering, Osaka University, Suita 565-0871, Japan*; orcid.org/0000-0002-2215-935X; Email: thayashi@chem.eng.osaka-u.ac.jp

Author

Yuta Miyazaki − *Department of Applied Chemistry, Graduate School of Engineering, Osaka University, Suita 565-0871, Japan*

Complete contact information is available at: https://pubs.acs.org/10.1021/acs.inorgchem.0c00901

Notes

The authors declare no competing financial interest.

■ ACKNOWLEDGMENTS

This work was financially supported by Grants-in-Aid for Scientific Research provided by JSPS KAKENHI Grant Numbers JP15H05804, JP16H06045, JP17J00008, JP18KK0156, and JP18K19099. We appreciate support from JST PRESTO (JPMJPR15S2). Y.M. appreciates support from the JSPS Research Fellowship for Young Scientists.

■ REFERENCES

(1) Ragsdale, S. W.; Raugei, S.; Ginovska, B.; Wongnate, T. Biochemistry of Methyl-Coenzyme M Reductase. In *The Biological Chemistry of Nickel*; Zamble, D., Rowińska-Żyrek, M., Kozlowski, H., Eds.; Royal Society of Chemistry: Cambridge, U.K., 2017; Chapter 8, p 149−169.

(2) Thauer, R. K. Methyl (Alkyl)-Coenzyme M Reductases: Nickel F-430-Containing Enzymes Involved in Anaerobic Methane Formation and in Anaerobic Oxidation of Methane or of Short Chain Alkanes. *Biochemistry* **2019**, *58*, 5198−5220.

(3) Ermler, U. On the mechanism of methyl-coenzyme M reductase. *Dalton Trans.* **2005**, 3451−3458.

(4) Evans, P. N.; Boyd, J. A.; Leu, A. O.; Woodcroft, B. J.; Parks, D. H.; Hugenholtz, P.; Tyson, G. W. An evolving view of methane metabolism in the Archaea. *Nat. Rev. Microbiol.* **2019**, *17*, 219−232.

(5) (a) Jaun, B.; Pfaltz, A. Coenzyme F430 from Methanogenic Bacteria: Reversible One-electron Reduction of F430 Pentamethyl Ester to the Nickel(I) Form. *J. Chem. Soc., Chem. Commun.* **1986**, 1327−1329. (b) Jaun, B. Coenzyme F430 from Methanogenic Bacteria: Oxidation of F430 Pentamethyl Ester to the Ni(III) Form. *Helv. Chim. Acta* **1990**, *73*, 2209−2217. (c) Piskorski, R.; Jaun, B. Direct Determination of the Number of Electrons Needed To Reduce Coenzyme F430 Pentamethyl Ester to the Ni(I) Species Exhibiting the Electron Paramagnetic Resonance and Ultraviolet-Visible Spectra Characteristic for the MCR_{red1} State of Methyl-coenzyme M Reductase. *J. Am. Chem. Soc.* **2003**, *125*, 13120−13125.

(6) (a) Krone, U. E.; Laufer, K.; Thauer, R. K.; Hogenkamp, H. P. C. Coenzyme F_{430} as a Possible Catalyst for the Reductive Dehalogenation of Chlorinated C1 Hydrocarbons in Methanogenic Bacteria. *Biochemistry* **1989**, *28*, 10061−10065. (b) Gantzer, C. J.; Wackett, L. P. Reductive Dechlorination Catalyzed by Bacterial Transition-Metal Coenzymes. *Environ. Sci. Technol.* **1991**, *25*, 715−722. (c) Holliger, C.; Schraa, G.; Stupperich, E.; Stams, A. J.; Zehnder, A. J. B. Evidence for the Involvement of Corrinoids and Factor F_{430} in the Reductive Dechlorination of 1,2-Dichloroethane by *Methanosarcina barkeri*. *J. Bacteriol.* **1992**, *174*, 4427−4434. (d) Holliger, C.; Kengen, S. W. M.; Schraa, G.; Stams, A. J. M.; Zehnder, A. J. B. Methyl-coenzyme M reductase of *Methanobacterium thermoautotrophicum* H Catalyzes the Reductive Dechlorination of 1,2-Dichloroethane to Ethylene and Chloroethane. *J. Bacteriol.* **1992**, *174*, 4435−4443.

(7) (a) Dey, M.; Kunz, R. C.; Lyons, D. M.; Ragsdale, S. W. Characterization of Alkyl-Nickel Adducts Generated by Reaction of Methyl-Coenzyme M Reductase with Brominated Acids. *Biochemistry* **2007**, *46*, 11969−11978. (b) Dey, M.; Telser, J.; Kunz, R. C.; Lees, N. S.; Ragsdale, S. W.; Hoffman, B. M. Biochemical and Spectroscopic Studies of the Electronic Structure and Reactivity of a Methyl-Ni Species Formed on Methyl-Coenzyme M Reductase. *J. Am. Chem. Soc.* **2007**, *129*, 11030−11032. (c) Yang, N.; Reiher, M.; Wang, M.; Harmer, J.; Duin, E. C. Formation of a Nickel-Methyl Species in Methyl-Coenzyme M Reductase, an Enzyme Catalyzing Methane Formation. *J. Am. Chem. Soc.* **2007**, *129*, 11028−11029. (d) Sarangi, R.; Dey, M.; Ragsdale, S. W. Geometric and Electronic Structures of the Ni^{I} and Methyl-Ni^{III} Intermediates of Methyl-Coenzyme M Reductase. *Biochemistry* **2009**, *48*, 3146−3156. (e) Kunz, R. C.; Horng, Y. C.; Ragsdale, S. W. Spectroscopic and Kinetic Studies of the Reaction of Bromopropanesulfonate with Methyl-coenzyme M Reductase. *J. Biol. Chem.* **2006**, *281*, 34663−34676.

(8) (a) Ermler, U.; Grabarse, W.; Shima, S.; Goubeaud, M.; Thauer, R. K. Crystal Structure of Methyl-Coenzyme M Reductase: The Key Enzyme of Biological Methane Formation. *Science* **1997**, *278*, 1457−1462. (b) Grabarse, W.; Mahlert, F.; Shima, S.; Thauer, R. K.; Ermler, U. Comparison of Three Methyl-coenzyme M Reductases from Phylogenetically Distant Organisms: Unusual Amino Acid Modification, Conservation and Adaptation. *J. Mol. Biol.* **2000**, *303*, 329−344. (c) Grabarse, W.; Mahlert, F.; Duin, E. C.; Goubeaud, M.; Shima, S.; Thauer, R. K.; Lamzin, V.; Ermler, U. On the Mechanism of Biological Methane Formation: Structural Evidence for Conformational Changes in Methyl-coenzyme M Reductase upon Substrate Binding. *J. Mol. Biol.* **2001**, *309*, 315−330. (d) Cedervall, P. E.; Dey, M.; Li, X.; Sarangi, R.; Hedman, B.; Ragsdale, S. W.; Wilmot, C. M. Structural Analysis of a Ni-Methyl Species in Methyl-Coenzyme M Reductase from *Methanothermobacter marburgensis*. *J. Am. Chem. Soc.* **2011**, *133*, 5626−5628.

(9) (a) Jaun, B.; Pfaltz, A. Coenzyme F430 from Methanogenic Bacteria: Methane Formation by Reductive Carbon-Sulfur Bond Cleavage of Methyl Sulphonium Ions Catalyzed by F430 Pentamethyl Ester. *J. Chem. Soc., Chem. Commun.* **1988**, 293−294. (b) Lin, S.-K.; Jaun, B. Coenzyme F430 from Methanogenic Bacteria: Detection of a Paramagnetic Methylnickel(II) Derivative of the Pentamethyl Ester by ^{2}H-NMR Spectroscopy. *Helv. Chim. Acta* **1991**, *74*, 1725−1738.

(10) (a) Stolzenberg, A. M.; Stershic, M. T. Reductive Chemistry of Nickel Hydroporphyrins: The Nickel(I) Octaethylisobacteriochlorin Anion. *Inorg. Chem.* **1987**, *26*, 3082−3083. (b) Stolzenberg, A. M.; Stershic, M. T. Reactions of the Nickel(I) Octaethylisobacteriochlorin Anion with Alkyl Halides. *J. Am. Chem. Soc.* **1988**, *110*, 5397−5403. (c) Stolzenberg, A. M.; Stershic, M. T. Reductive Chemistry of Nickel Hydroporphyrins. Evidence for a Biologically Significant Difference between Porphyrins, Hydroporphyrins, and Other Tetrapyrroles. *J. Am. Chem. Soc.* **1988**, *110*, 6391−6402. (d) Lahiri, G. K.; Schussel, L. J.; Stolzenberg, A. M. F430 Model Chemistry. Mechanistic Investigation of the Reduction, Coupling, and Dehydrohalogenation of Alkyl Halides by the Nickel(I) Octaethylisobacteriochlorin Anion. *Inorg. Chem.* **1992**, *31*, 4991−5000. (e) Lahiri, G. K.; Stolzenberg, A. M. F430 Model Chemistry. Evidence for Alkyl- and Hydrido-Nickel Intermediates in the Reactions of the Nickel(I) Octaethylisobacteriochlorin Anion. *Inorg. Chem.* **1993**, *32*, 4409−4413.

(11) Helvenston, M. C.; Castro, C. E. Nickel(I) Octaethylisobacteriochlorin Anion. An Exceptional Nucleophile. Reduction and Coupling of Alkyl Halides by Anionic and Radical Processes. A Model for Factor F-430. *J. Am. Chem. Soc.* **1992**, *114*, 8490−8496.

(12) (a) D'Aniello, M. J.; Barefield, E. K. A Paramagnetic, Square-Pyramidal Nickel(II) Alkyl Complex. *J. Am. Chem. Soc.* **1976**, *98*, 1610−1611. (b) Gosden, C.; Healy, K. P.; Pletcher, D. Reaction of Electrogenerated Square-planar Nickel(I) Complexes with Alkyl Halides. *J. Chem. Soc., Dalton Trans.* **1978**, 972−976.

(13) (a) Pelmenschikov, V.; Blomberg, M. R. A.; Siegbahn, P. E. M.; Crabtree, R. H. A Mechanism from Quantum Chemical Studies for Methane Formation in Methanogenesis. *J. Am. Chem. Soc.* **2002**, *124*, 4039−4049. (b) Pelmenschikov, V.; Siegbahn, P. E. M. Catalysis by

methyl-coenzyme M reductase: a theoretical study for heterodisulfide product formation. *JBIC, J. Biol. Inorg. Chem.* **2003**, *8*, 653−662. (c) Chen, S.-L.; Pelmenschikov, V.; Blomberg, M. R. A.; Siegbahn, P. E. M. Is There a Ni-Methyl Intermediate in the Mechanism of Methyl-Coenzyme M Reductase? *J. Am. Chem. Soc.* **2009**, *131*, 9912−9913. (d) Chen, S.-L.; Blomberg, M. R. A.; Siegbahn, P. E. M. How Is Methane Formed and Oxidized Reversibly When Catalyzed by Ni-Containing Methyl-Coenzyme M Reductase? *Chem. - Eur. J.* **2012**, *18*, 6309−6315. (e) Chen, S.-L.; Blomberg, M. R. A.; Siegbahn, P. E. M. An investigation of possible competing mechanisms for Ni-containing methyl−coenzyme M reductase. *Phys. Chem. Chem. Phys.* **2014**, *16*, 14029−14035.

(14) Wongnate, T.; Sliwa, D.; Ginovska, B.; Smith, D.; Wolf, M. W.; Lehnert, N.; Raugei, S.; Ragsdale, S. W. The radical mechanism of biological methane synthesis by methyl-coenzyme M reductase. *Science* **2016**, *352*, 953−958.

(15) (a) Furenlid, L. R.; Renner, M. W.; Smith, K. M.; Fajer, J. Structural Consequences of Nickel versus Macrocycle Reductions in F430 Models: EXAFS Studies of a Ni(I) Anion and Ni(II) n Anion Radicals. *J. Am. Chem. Soc.* **1990**, *112*, 1634−1635. (b) Renner, M. W.; Furenlid, L. R.; Barkigia, K. M.; Forman, A.; Shim, H.-K.; Simpson, D. J.; Smith, K. M.; Fajer, J. Models of Factor 430. Structural and Spectroscopic Studies of Nickel(II) and Nickel(I) Hydroporphyrins. *J. Am. Chem. Soc.* **1991**, *113*, 6891−6898.

(16) (a) Bakac, A.; Espenson, J. H. Kinetics and Mechanism of the Alkylnickel Formation in One-Electron Reductions of Alkyl Halides and Hydroperoxides by a Macrocyclic Nickel(I) Complex. *J. Am. Chem. Soc.* **1986**, *108*, 713−719. (b) Ram, M. S.; Bakac, A.; Espenson, J. H. Free-Radical Pathways to Alkyl Complexes of a Nickel Tetraaza Macrocycle. *Inorg. Chem.* **1986**, *25*, 3267−3272. (c) Bakac, A.; Espenson, J. H. Mechanistic Investigation of Carbon-Carbon Bond Formation in the Reduction of Alkyl Halides by Organonickel Complexes in Aqueous Solution. *J. Am. Chem. Soc.* **1986**, *108*, 719−723.

(17) Nishigaki, J.; Matsumoto, T.; Tatsumi, K. Model Studies of Methyl CoM Reductase: Methane Formation via CH_3−S Bond Cleavage of Ni(I) Tetraazacyclic Complexes Having Intramolecular Methyl Sulfide Pendants. *Inorg. Chem.* **2012**, *51*, 5173−5187.

(18) Brenig, C.; Prieto, L.; Oetterli, R.; Zelder, F. A Nickel(II)-Containing Vitamin B_{12} Derivative with a Cofactor-F430-type π-System. *Angew. Chem., Int. Ed.* **2018**, *57*, 16308−16312.

(19) Oohora, K.; Onoda, A.; Hayashi, T. Hemoproteins Reconstituted with Artificial Metal Complexes as Biohybrid Catalysts. *Acc. Chem. Res.* **2019**, *52*, 945−954.

(20) (a) Oohora, K.; Miyazaki, Y.; Hayashi, T. Myoglobin Reconstituted with Ni Tetradehydrocorrin as a Methane-Generating Model of Methyl-coenzyme M Reductase. *Angew. Chem., Int. Ed.* **2019**, *58*, 13813−13817. (b) Miyazaki, Y.; Oohora, K.; Hayashi, T. Methane generation via intraprotein C−S bond cleavage in cytochrome b_{562} reconstituted with nickel didehydrocorrin. *J. Organomet. Chem.* **2019**, *901*, 120945.

(21) Lin, S.-K.; Jaun, B. Coenzyme F430 from Methanogenic Bacteria: Mechanistic Studies on the Reductive Cleavage of Sulfonium Ions Catalyzed by F430 Pentamethyl Ester Helv. *Helv. Chim. Acta* **1992**, *75*, 1478−1490.

(22) (a) Cedervall, P. E.; Dey, M.; Pearson, A. R.; Ragsdale, S. W.; Wilmot, C. M. Structural Insight into Methyl-Coenzyme M Reductase Chemistry Using Coenzyme B Analogues. *Biochemistry* **2010**, *49*, 7683−7693. (b) Ebner, S.; Jaun, B.; Goenrich, M.; Thauer, R. K.; Harmer, J. Binding of Coenzyme B Induces a Major Conformational Change in the Active Site of Methyl-Coenzyme M Reductase. *J. Am. Chem. Soc.* **2010**, *132*, 567−575. (c) Wongnate, T.; Ragsdale, S. W. The Reaction Mechanism of Methyl-Coenzyme M Reductase HOW AN ENZYME ENFORCES STRICT BINDING ORDER. *J. Biol. Chem.* **2015**, *290*, 9322−9334.

(23) The benzyl group appears to be added at the meso positions of TDHC ligand via transbenzylation from the nickel center because the meso position of porphyrinoid is highly electrophilic. The generated transient benzyl anion species could easily be transferred to the meso position. Moreover, the benzyl group adduct of Ni(TDHC) should be inactive toward reduction with dithionite because its macrocycle is highly saturated, and the redox potential of the Ni^{II}/Ni^{I} is expected to be negatively shifted compared to that of Ni(TDHC) as reported in ref 20b.

(24) (a) Kalisch, W. W.; Senge, M. O. Facile *meso* Functionalization of Porphyrins by Nucleophilic Substitution with Organolithium Reagents. *Angew. Chem., Int. Ed.* **1998**, *37*, 1107−1109. (b) Senge, M. O.; Kalisch, W. W.; Bischoff, I. The Reaction of Porphyrins with Organolithium Reagents. *Chem. - Eur. J.* **2000**, *6*, 2721−2738.

(25) (a) Gruber, K.; Puffer, B.; Kräutler, B. Vitamin B_{12}-derivatives-enzyme cofactors and ligands of proteins and nucleic acids. *Chem. Soc. Rev.* **2011**, *40*, 4346−4363. (b) Giedyk, M.; Goliszewska, K.; Gryko, D. Vitamin B_{12} catalysed reactions. *Chem. Soc. Rev.* **2015**, *44*, 3391−3404.

(26) (a) Hayashi, T.; Morita, Y.; Mizohata, E.; Oohora, K.; Ohbayashi, J.; Inoue, T.; Hisaeda, Y. Co(II)/Co(I) reduction-induced axial histidine-flipping in myoglobin reconstituted with a cobalt tetradehydrocorrin as a methionine synthase model. *Chem. Commun.* **2014**, *50*, 12560−12563. (b) Morita, Y.; Oohora, K.; Sawada, A.; Doitomi, K.; Ohbayashi, J.; Kamachi, T.; Yoshizawa, K.; Hisaeda, Y.; Hayashi, T. Intraprotein transmethylation *via* a CH_3−Co(III) species in myoglobin reconstituted with a cobalt corrinoid complex. *Dalton Trans.* **2016**, *45*, 3277−3284. (c) Morita, Y.; Oohora, K.; Sawada, A.; Kamachi, T.; Yoshizawa, K.; Hayashi, T. Redox Potentials of Cobalt Corrinoids with Axial Ligands Correlate with Heterolytic Co−C Bond Dissociation Energies. *Inorg. Chem.* **2017**, *56*, 1950−1955.

(27) (a) Rusling, J. F.; Zhou, D.-L. Electrochemical catalysis in microemulsions. Dynamics and organic synthesis. *J. Electroanal. Chem.* **1997**, *439*, 89−96. (b) Shey, J.; McGinley, C. M.; McCauley, K. M.; Dearth, A. S.; Young, B. T.; van der Donk, W. A. Mechanistic Investigation of a Novel Vitamin B_{12}-Catalyzed Carbon-Carbon Bond Forming Reaction, the Reductive Dimerization of Arylalkenes. *J. Org. Chem.* **2002**, *67*, 837−846. (c) Hisaeda, Y.; Tahara, K.; Shimakoshi, H.; Masuko, T. Bioinspired catalytic reactions with vitamin B_{12} derivative and photosensitizers. *Pure Appl. Chem.* **2013**, *85*, 1415−1426. (d) Giedyk, M.; Fedosov, S. N.; Gryko, D. An amphiphilic, catalytically active, vitamin B_{12} derivative. *Chem. Commun.* **2014**, *50*, 4674−4676.

(28) There is possibility that the inactivation reaction to form the benzyl-cofactor adduct suppresses the homocoupling product in the case of rMb(Ni^{I}(TDHC)) showing the low TON value. However, the inactivation is considered to be insignificant because the non-negligible amount of the homocoupling product was obtained by rMb(Co^{I}(TDHC)) with the similar low total TON values to that of rMb(Ni^{I}(TDHC)).

(29) Although we also employed *p*-methoxybenzyl bromide, the yield of the corresponding product, *p*-methoxytoluene, was below the detection limit of GC/MS.

(30) σ_P and σ_P^- are classical and resonance-responsive Hammett substituent constants for *para*-substituted aryl derivatives described in a previous report: Hansch, C.; Leo, A.; Taft, R. W. A Survey of Hammett Substituent Constants and Resonance and Field Parameters. *Chem. Rev.* **1991**, *91*, 165−195.

(31) $\sigma_J^\bullet$ is Jackson's spin-delocalization substituent constant for *para*-substituted aryl derivatives described in a previous report: Ağirbaş, H.; Jackson, R. A. Free Radical Reactions in Solution. Part 9. Further **σ02D9** Values from Decomposition of Substituted Dibenzylmercurials. *J. Chem. Soc., Perkin Trans. 2* **1983**, *2*, 739−742.

(32) $\sigma_{JJ}^\bullet$ is Jiang's spin-delocalization substituent constant for *para*-substituted aryl derivatives described in a previous report: Jiang, X.-K.; Ji, G.-Z. A Self-Consistent and Cross-Checked Scale of Spin-Delocalization Substituent Constants, the $\dot{\sigma}_{JJ}$ Scale. *J. Org. Chem.* **1992**, *57*, 6051−6056.

(33) Creary's $\sigma_C^\bullet$ spin-delocalization substituent constant for *para*-substituted aryl derivatives are categorized in two sets which were determined in the thermal rearrangement of 1,1-dimethyl-2-methylenecyclopropanes in C_6D_6 at 80 °C (parameter set 1) and in isooctane at 100 °C (parameter set 2) as reported in ref 33. In the

https://dx.doi.org/10.1021/acs.inorgchem.0c00901
Inorg. Chem. XXXX, XXX, XXX−XXX

present report, we employed values of parameter set 2 as Creary's $\sigma_C^\bullet$ spin-delocalization substituent constants because of the high correlation with the data.

(34) (a) Creary, X.; Mehrsheikh-Mohammadi, M. E.; McDonald, S. Methylenecyclopropane Rearrangement as a Probe for Free Radical Substituent Effects. $\dot{\sigma}$ Values for Commonly Encountered Conjugating and Organometallic Groups. *J. Org. Chem.* **1987**, *52*, 3254−3263. (b) Creary, X. Super Radical Stabilizers. *Acc. Chem. Res.* **2006**, *39*, 761−771.

(35) $\sigma_\beta^\bullet$ is Arnold's spin-delocalization substituent constant for *para*-substituted aryl derivatives described in a previous report: Dust, J. M.; Arnold, D. R. Substituent Effects on Benzyl Radical ESR Hyperfine Coupling Constants. The $\sigma_\beta^\bullet$ Scale Based upon Spin Delocalization. *J. Am. Chem. Soc.* **1983**, *105*, 1221−1227.

(36) $\sigma_F^\bullet$ is Fisher's spin-delocalization substituent constant for *para*-substituted aryl derivatives described in a previous report: Fisher, T. H.; Meierhoefer, A. W. Substituent Effects in Free-Radical Reactions. A Study of 4-Substituted 3-Cyanobenzyl Free Radicals. *J. Org. Chem.* **1978**, *43*, 224−228.

(37) The set of "ρ^X and σ^X" represents "polar substituent constant and corresponding reaction constant", and the set of "$\rho^\bullet$ and $\sigma^\bullet$" represents "spin-delocalization substituent constant and corresponding reaction constant".

(38) (a) Jiang, X.-K. Establishment and Successful Application of the $\sigma_{JJ}^\bullet$ Scale of Spin-Delocalization Substituent Constants. *Acc. Chem. Res.* **1997**, *30*, 283−289. (b) Kim, S. S.; Zhu, Y.; Lee, K. H. Thermal Isomerizations of Ketenimines to Nitriles: Evaluations of Sigma-Dot ($\sigma^\bullet$) Constants for Spin-Delocalizations. *J. Org. Chem.* **2000**, *65*, 2919−2923. (c) Liu, J.; Hu, L.; Wang, L.; Chen, H.; Deng, L. An Iron(II) Ylide Complex as a Masked Open-Shell Iron Alkylidene Species in Its Alkylidene-Transfer Reactions with Alkenes. *J. Am. Chem. Soc.* **2017**, *139*, 3876−3888. (d) Carminati, D. M.; Fasan, R. Stereoselective Cyclopropanation of Electron-Deficient Olefins with a Cofactor Redesigned Carbene Transferase Featuring Radical Reactivity. *ACS Catal.* **2019**, *9*, 9683−9697. (e) Cailler, L. P.; Clémancey, M.; Barilone, J.; Maldivi, P.; Latour, J.-M.; Sorokin, A. B. Comparative Study of the Electronic Structures of μ-Oxo, μ-Nitrido, and μ-Carbido Diiron Octapropylporphyrazine Complexes and Their Catalytic Activity in Cyclopropanation of Olefins. *Inorg. Chem.* **2020**, *59*, 1104−1116.

(39) σ_{mb} is Jiang's polar substituent constant for *para*-substituted aryl derivatives described in a previous report: Ji, G.-Z.; Jiang, X.-K.; Zhang, Y.-H.; Yuan, S.-G.; Yu, C.-X.; Shi, Y.-Q.; Zhang, X.-L.; Shi, W.-T. The spin delocalization substitutent parameter $\dot{\sigma}_{JJ}$. 5. Correlation analysis of ^{19}F chemical shifts of substituted trifluorostyrenes. The unresolved polar substituent parameter σ_{mb}. *J. Phys. Org. Chem.* **1990**, *3*, 643−650.

(40) (a) Brennan, M. R.; Kim, D.; Fout, A. R. A synthetic and mechanistic investigation into the cobalt(I) catalyzed amination of aryl halides. *Chem. Sci.* **2014**, *5*, 4831−4839. (b) Arrechea, P. L.; Buchwald, S. L. Biaryl Phosphine Based Pd(II) Amido Complexes: The Effect of Ligand Structure on Reductive Elimination. *J. Am. Chem. Soc.* **2016**, *138*, 12486−12493.

(41) (a) Key, H. M.; Dydio, P.; Clark, D. S.; Hartwig, J. F. Abiological catalysis by artificial haem proteins containing noble metals in place of iron. *Nature* **2016**, *534*, 534−537. (b) Key, H. M.; Dydio, P.; Liu, Z.; Rha, J. Y.-E.; Nazarenko, A.; Seyedkazemi, V.; Clark, D. S.; Hartwig, J. F. Beyond Iron: Iridium-Containing P450 Enzymes for Selective Cyclopropanations of Structurally Diverse Alkenes. *ACS Cent. Sci.* **2017**, *3*, 302−308.

(42) (a) Sreenilayam, G.; Moore, E. J.; Steck, V.; Fasan, R. Metal Substitution Modulates the Reactivity and Extends the Reaction Scope of Myoglobin Carbene Transfer Catalysts. *Adv. Synth. Catal.* **2017**, *359*, 2076−2089. (b) Moore, E. J.; Steck, V.; Bajaj, P.; Fasan, R. Chemoselective Cyclopropanation over Carbene Y-H Insertion Catalyzed by an Engineered Carbene Transferase. *J. Org. Chem.* **2018**, *83*, 7480−7490.

(43) Wolf, M. W.; Vargas, D. A.; Lehnert, N. Engineering of RuMb: Towards a Green Catalyst for Carbene Insertion Reactions. *Inorg. Chem.* **2017**, *56*, 5623−5635.

(44) Oohora, K.; Meichin, H.; Zhao, L.; Wolf, M. W.; Nakayama, A.; Hasegawa, J.; Lehnert, N.; Hayashi, T. Catalytic Cyclopropanation by Myoglobin Reconstituted with Iron Porphycene: Acceleration of Catalysis due to Rapid Formation of the Carbene Species. *J. Am. Chem. Soc.* **2017**, *139*, 17265−17268.

(45) Covington, A. K.; Paabo, M.; Robinson, R. A.; Bates, R. G. Use of the Glass Electrode in Deuterium Oxide and the Relation between the Standardized pD (pa_D) Scale and the Operational pH in Heavy Water. *Anal. Chem.* **1968**, *40*, 700−706.

https://dx.doi.org/10.1021/acs.inorgchem.0c00901
Inorg. Chem. XXXX, XXX, XXX−XXX